Vibration control with self-tuning vibration absorption employing Extremum seeking algorithm

D. E. Casagrande [1], P. Gardonio [2], G. Konda Rodrigues [2]
[1] Universidad de O'Higgins, Instituto de Ciencias de la Ingeniería,
Libertador O'Higgins 611, 2820000, Rancagua, Chile
e-mail: **daniel.casagrande@uoh.cl**

[2] Università degli Studi di Udine, DPIA,
Via delle Scienze 206, 33100, Udine, Italy

Abstract
This paper presents a simulation study on the control performance of a self-tuning vibration absorber. The study considers a tuneable vibration absorber, composed by a spring-mass-damper system with variable stiffness and damping components, which is attached to a single degree of freedom mechanical system subjected to a harmonic excitation. The online tuning of the stiffness and damping parameters is performed using an extremum seeking algorithm set to minimize the vibration kinetic energy of the hosting system. Starting from initial estimates of the stiffness and damping components of the absorber, the extremum seeking algorithm is implemented simultaneously on both variables until the optimal values are found. The study shows that the proposed tuning approach efficiently converges to the optimal stiffness and damping parameters of the absorber that would minimise the response of the hosting system due to tonal excitations.

1 Introduction

This paper presents a simulation study that investigates the use of an extremum seeking algorithm to tune the damping and stiffness parameters of a vibration absorber attached to a Single-Degree-Of-Freedom (SDOF) structure which is subject to a harmonic excitation. Vibration absorbers first recorded propositions appeared in a 1883 conference paper authored by Watts [1] and a patent filed by a German engineer in 1909 [2]; and their mathematical formulation was presented in 1928 in a seminal work by Ormondroyd and Den Hartog [3]. These devices are known under several names, such as Dynamic Vibration Absorbers, Tuned Mass Damper, Vibration Neutraliser, and Tuned Vibration Absorbers (TVA)[4]–[6]; but the key concept is that they are composed of a seismic mass mounted on the structure via a spring-damper system whose parameters are carefully chosen such that the TVA couples with the mechanical system to attenuate its vibration at target frequencies [4].

This type of devices can tackle two different vibration control problems depending on whether the hosting structure is subject to tonal or to broad frequency band disturbances. In their work, Ormondroyd and Den Hartog [3], proposed that, for broad frequency band disturbances, the natural frequency of the absorber should be tuned to the resonance frequency of the controlled mode and its damping component should be tuned minimise the broadband response of that mode. They proved that the damping element not only dissipates energy but increases the frequency range over which the absorber is effective [3]. Instead, if the aim is to reduce the amplitude of the harmonic response due to a tonal disturbance, the absorber natural frequency should be tuned to the frequency of the forcing signal and its damping component should be as low as possible, considering that there is a trade-off between the TVA mass and its displacement [4].

In any case, the fine tuning of the TVA stiffness and damping parameters, especially the stiffness for tonal disturbances, is crucial to attain good vibration control performances. Poor vibration reductions or even increased vibrations due to mistuning of the TVA is one of the most common implementation problems,

particularly when the natural frequencies of the hosting structure shift upwards or downwards due to changes in the environmental or operational conditions such as temperature or load changes. To tackle this issue, many studies propose the use of adaptive TVAs in which diverse strategies haven been devised to enable the adjustment of the vibration absorber parameters to maintain an optimal tuning. One approach is to use electromechanical vibration absorbers instead of purely mechanical ones, e.g., shunted piezoelectric strain [7]–[12] or seismic electromagnetic transducers [13]–[17] so that by changing the electrical parameters of the transducers it is possible to tune the TVA to specific target frequencies.

In recent studies, adaptive controllers based on extremum seeking algorithms were implemented to tune the parameters of vibration absorbers subject to broad frequency band disturbances [18], [19]. These algorithms relay on a perturb-and-observe approach, which is used to maximise a metric of the system performance with respect to one or more of its parameters [20]. Extremum seeking algorithms need an initial guess of the variable whose optimum is being searched and a cost function which represents the metric being maximised. Initially, they were used for controlling hard-to-model systems, in which static cost functions were employed [21], [22]. But, more recently, the use of dynamic cost functions has been investigated too [20], [23]. In [19], the cost function that is maximised by the extremum seeking algorithm is the power absorbed by the electrical shunt connected to a piezoelectric vibration absorber.

In this work, an extremum seeking algorithm is implemented to simultaneously tune the stiffness and damping components of the TVA attached to SDOF structure subject to a sinusoidal excitation force. In particular, the extremum seeking algorithm is set to minimise the instantaneous kinetic energy of the hosting structure. The kinetic energy of the structure is also used to assess the performance of the vibration absorber.

The study considers 3 different scenarios regarding the excitation force. The first one considers a tonal signal whose frequency is below the natural frequency of the structure. The second one is when the excitation frequency matches the structure natural frequency, and the third one is when the forcing frequency is above the natural frequency of the structure.

The paper is structured in two main sections. Section 2 presents the SDOF model, the mathematical formulation and the control strategy implemented in the simulation study. Section 3 reports the performance results of the proposed self-tuning vibration absorber and a study on the impact of the inherent parameters of the extremum seeking algorithm on the algorithm convergence speed and stability.

2 Model problem

This section presents the model of the SDOF hosting system equipped with the TVA and the mathematical formulation used to obtain the kinetic energy of the hosting system, which is used both as a cost function to find the optimal stiffness and damping parameters of the TVA and to assess the performance of the absorber.

2.1 SDOF system and TVA

Figure 1 shows the whole setup, which is composed of a mass-spring-damper SDOF hosting system equipped with a mechanical vibration absorber characterised by variable damping and stiffness components. The hosting system is subject to a tonal excitation force $f_s(t)$.

$$f_s = f_0 \sin(\omega_0 t) \, . \tag{1}$$

The equations of motions of the hosting system and TVA masses are derived below, where the time dependence has been omitted for simplicity:

$$m_s \ddot{y}_s + (c_s + c_a)\dot{y}_s + (k_s + k_a)y_s - c_a \dot{y}_a - k_a y_a \; = f_s \, , \tag{2}$$

$$m_a \ddot{y}_a + c_a \dot{y}_a + k_a y_a - c_a \dot{y}_s - k_a y_s \; = 0 \, . \tag{3}$$

Here m_s, k_s, c_s, m_a, k_a and c_a are the mass, stiffness and damping of the structure and of the absorber respectively; and y_s, $\dot{y}_s$, $\ddot{y}_s$, y_a, $\dot{y}_a$, $\ddot{y}_a$ are the displacement, velocity and acceleration of the structure mass and of the absorber mass respectively.

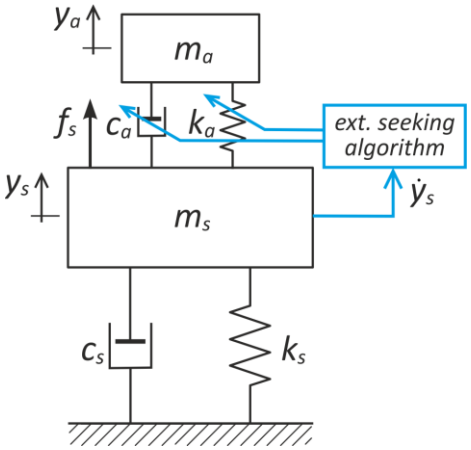

Figure 1: Model of the system.

Equations (2) and (3) can be casted into a matrix state space form as

$$\dot{\mathbf{x}} = \mathbf{A}\mathbf{x} + \mathbf{B}f_s \tag{4}$$

where **x** is the state vector, **A** is the state matrix and **B** is the input vector, which are given by

$$\mathbf{x} = \begin{bmatrix} y_s \\ y_a \\ \dot{y}_s \\ \dot{y}_a \end{bmatrix}, \quad A = \begin{bmatrix} 0 & 0 & 1 & 0 \\ 0 & 0 & 0 & 1 \\ -\frac{k_s+k_a}{m_s} & \frac{k_a}{m_s} & -\frac{c_s+c_a}{m_s} & \frac{c_a}{m_s} \\ \frac{k_a}{m_a} & -\frac{k_a}{m_a} & \frac{c_a}{m_a} & -\frac{c_a}{m_a} \end{bmatrix}, \quad \text{and} \quad \mathbf{B} = \begin{bmatrix} 0 \\ 0 \\ \frac{f_s}{m_s} \\ 0 \end{bmatrix}. \tag{5}$$

The response of the hosting system is evaluated with respect to its kinetic energy, which is given by:

$$K(t) = \frac{1}{2} m_s \dot{y}_s^2 \, . \tag{6}$$

The velocity of the hosting system mass and of the absorber mass can be retrieved from the state vector using

$$\dot{y}_s = \mathbf{C}_\mathrm{K}\mathbf{x} \, , \quad \dot{y}_a = \mathbf{C}_\mathrm{A}\mathbf{x} \, , \tag{7}$$

where the output matrix $\mathbf{C}_\mathrm{K}$ and $\mathbf{C}_\mathrm{A}$ are defined as

$$\mathbf{C}_\mathrm{K} = [0 \quad 0 \quad 1 \quad 0] \, , \quad \mathbf{C}_\mathrm{A} = [0 \quad 0 \quad 0 \quad 1] \, . \tag{8}$$

Using equations 7 and 8, the kinetic energy can be expressed as

$$K(t) = \frac{1}{2} m_s \mathbf{x}^\mathrm{T} \mathbf{C}_\mathrm{K}^\mathrm{T} \mathbf{C}_\mathrm{K} \mathbf{x} \, . \tag{9}$$

To assess the performance of the controller, the time-average kinetic energy of the system $\overline{K}$ was obtained offline performing a centered moving average that uses a sliding window of one second.

2.2 Extremum seeking tuning algorithm

The tuning of the absorber stiffness and damping components is achieved using an extremum seeking gradient search algorithm that minimizes the cost function, which in this study is the kinetic energy K of the structure presented in Eq. (9). The block diagram of the system state space model and the extremum seeking algorithms used to tune the absorber stiffness and damping is shown in Figure 2. The extremum seeking algorithm needs an initial guess of the damping c_a and stiffness k_a values to start the search, and in this study the tuning of both parameters is performed simultaneously. The instantaneous kinetic energy of the system is fed to the control feedback loops, which continuously modify c_a and k_a until they converge to the values that minimize the response of the system.

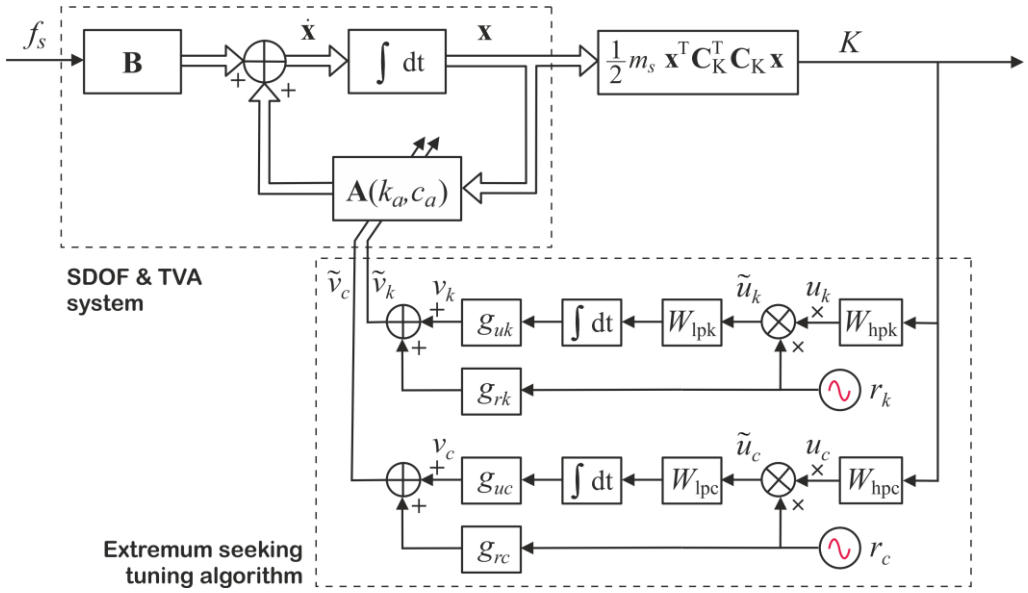

Figure 2: Block diagram of the state space model of the system with the extremum seeking gradient search feedback control loop for the online tuning of the TVA stiffness and damping components.

The extremum seeking algorithm is a perturb-and-observe type of controller whose general working principle will be briefly explained here. The subscripts k and c used to identify the extremum seeking signals for each feedback control loop are omitted as the explanation is valid for both feedback loops. The algorithm is based on the perturbation of the signal being optimized, in this study $K(t)$, using a low frequency sinusoidal signal $r(t)$. This ripple signal is amplified by a gain g_r and added to the feedback signal $v(t)$ to obtain the real-time value of the stiffness or damping component $\tilde{v}(t)$ implemented by the absorber as

$$\tilde{v}(t) = v(t) + g_r r(t)\,, \tag{10}$$

which is characterized by a time-harmonic ripple too.

Extremum seeking gradient search algorithms are used to maximize the value of a cost function with respect to a particular parameter of the system. In this case, as the goal is to minimize the kinetic energy of the hosting system, a negative feedback loop is implemented. After this gain is applied, the kinetic energy signal $K(t)$ is expected to be in-phase with the sinusoidal signal $r(t)$ when $v(t)$ is below the optimal stiffness or damping value, and these two signals are expected to be out-of-phase when $v(t)$ is above the optimal value. Therefore, it is sufficient to check the relative phase of the signals $r(t)$ and $K(t)$ to determine if the tuning signal $v(t)$ should increase or decrease. To do this, low-frequency components of the kinetic energy signal $K(t)$ are removed using a high-pass filter W_{hp} with a proper cut-off frequency. And to compare the phase of the of the reference signal $r(t)$ with the filtered signal $u(t)$, the controller multiplies these two signals to obtain $\tilde{u}(t)$, which is then filtered with a low pass filter W_{lp} to focus on the low-frequency phase difference of the compared signals. If they are in phase, the signal $\tilde{u}(t)$ will be a mostly positive wavy signal, otherwise it will be a mostly negative wavy signal. Then, the tuning signal $v(t)$ is obtained by rectifying the wavy signal

$$v(t) = g_u \int \tilde{u}(t)\mathrm{d}t\,. \tag{11}$$

In conclusion, the tuning signal will tend to rise if it is lower than the optimal stiffness or damping value and tend to decrease if it is higher than the optimal value. The control performance of the implemented strategy and how each parameter of the extremum seeking feedback control loop affects the convergence speed and stability will be discussed in the following section.

3 TVA online tuning implementation

The performance of the control system is analyzed for three different force excitation frequencies ω_0 with respect to the hosting system natural frequency $\omega_s = \sqrt{k_s/m_s}$: 1) $\omega_0 = 0.5\omega_s$, 2) $\omega_0 = \omega_s$ and 3) $\omega_0 = 1.5\omega_s$. To assess the behavior and performance of the controller, the time history of the structure and absorber mass velocities, of the kinetic energy and of the absorber stiffness and damping parameters are shown for the three cases, together with the frequency response of the structure implementing the optimal stiffness and damping of the TVA found by the extremum seeking algorithm.

This section also includes a convergence analysis of the control algorithm considering a simplified system in which the absorber damping value remains constant and the stiffness is optimized. This analysis brings insights on how the intrinsic parameters of extremum seeking algorithm affect the stability and convergence speed of the algorithm.

3.1 Control performance

The physical parameters of the system considered for this simulation study are reported in Table 1. The natural frequency and the damping ratio of the hosting system are fixed at 140 Hz and 5% respectively. The mass of the absorber is fixed at 25% the mass of the structure. As already mentioned, three cases are analyzed, and considering that the structure natural frequency is 140 Hz the input frequency for each case is equal to 70 Hz, 140 Hz and 210 Hz respectively.

Additionally, the extremum seeking feedback control loops must be configured. There are 6 parameters for each loop: the ripple signal $r(t)$ amplitude and frequency, the high-pass filter cut-off frequency, the low-pass filter cut-off frequency, the ripple gain, and the tuning signal gain. Table 2 presents the values used to configure each loop for the three cases. If for one parameter different values are used for the three simulation cases, the three value are shown between brackets and separated by a comma, i.e. (case 1, case 2, case 3).

Table 1: Parameters of the structure and TVA used in the simulation study.

Parameter	Symbol	Value	Units
Mass of the structure	m_s	0.3	kg
Natural frequency of the structure	ω_s	879.6	rad/s
Stiffness of the structure	k_s	232.1	N/m
Damping ratio of the structure	ζ_s	0.05	---
Damping of the structure	c_s	26.4	Ns/m
Mass of the absorber	m_a	0.075	kg

Table 2: Structure and absorber parameters used in the simulation study.

Parameter	Symbol	Damping control loop	Stiffness control loop
Ripple signal amplitude	A_r	0.1	100
Ripple gain	g_r	1	(2, 10, 10)
Tuning signal gain	g_u	(2e8, 1e8, 11e8)	(9e7, 7e7, 15e8)
Ripple signal frequency	ω_r	6π	2π
High-pass filter cut-off frequency	ω_{hp}	3π	π
Low-pass filter cut-off frequency	ω_{lp}	0.55	0.2

Finally, the initial values of the TVA stiffness and damping should also be guessed. The initial damping value of the TVA is set in all three cases to a relatively high value, considering that for a harmonic excitation the optimum TVA damping value tends to zero [24]. Instead, for the initial guess of the absorber stiffness different starting conditions are considered. For the first case, when $\omega_0 = 0.5\omega_s$, the initial guess is set to a value such that the TVA is tuned to half the input frequency, i.e. $k_a = m_a(0.5\omega_0)^2$. In cases 2 and 3, when $\omega_0 = \omega_s$ and $\omega_0 = 1.5\omega_s$, the initial guess for the stiffness is set to $k_a = m_a(1.5\omega_0)^2$. Before conducting the simulation study, the optimum stiffness value was found for each case.

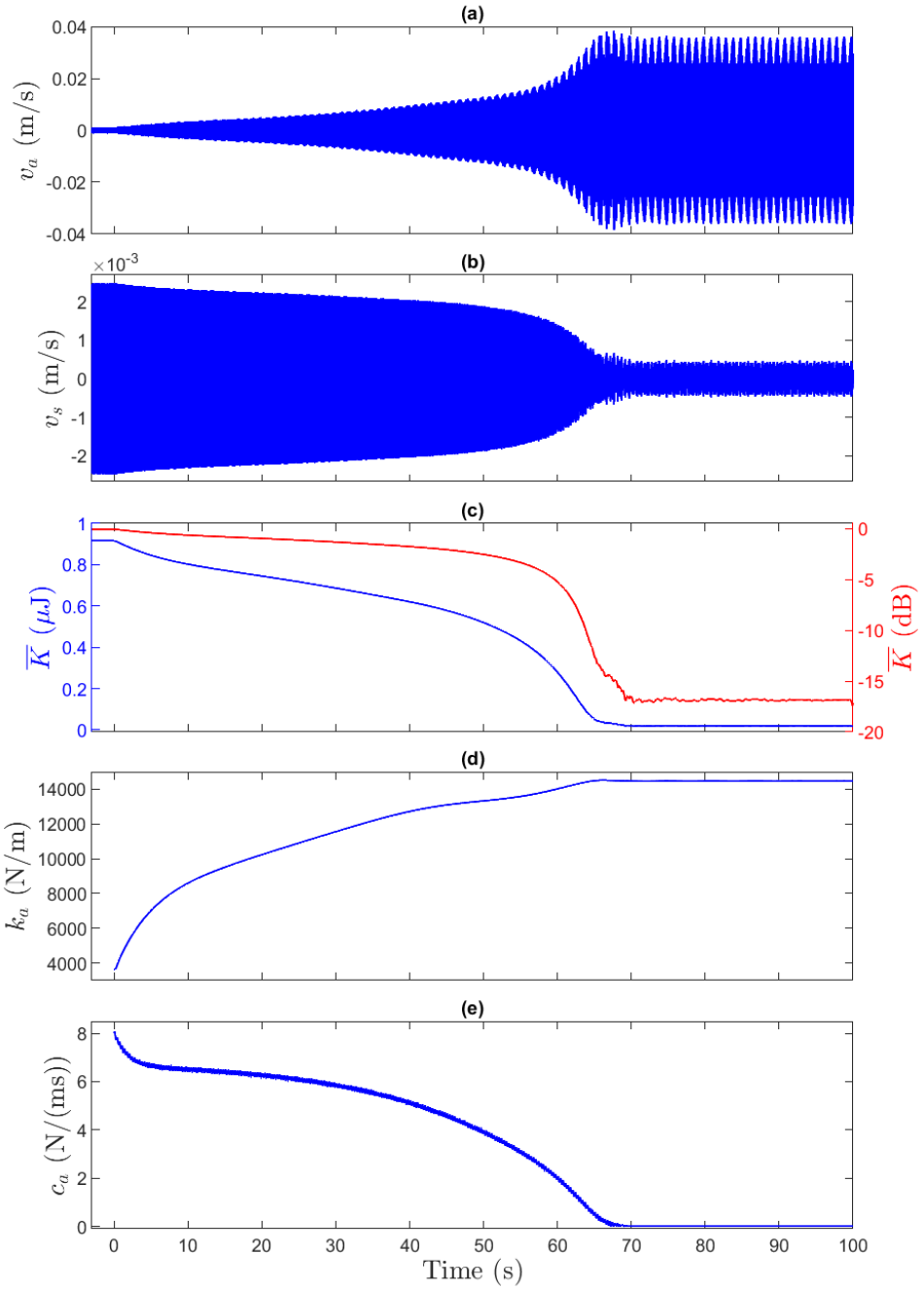

Figure 3: Time domain response of the system for the case 1: $\omega_0 = 0.5\omega_s$. (a) velocity of the TVA mass, (b) velocity of the structure mass, (c) time-average kinetic energy absolute value (blue line) and dB reduction with reference to its initial value (red line), (d) stiffness of the TVA, and (e) damping of the TVA.

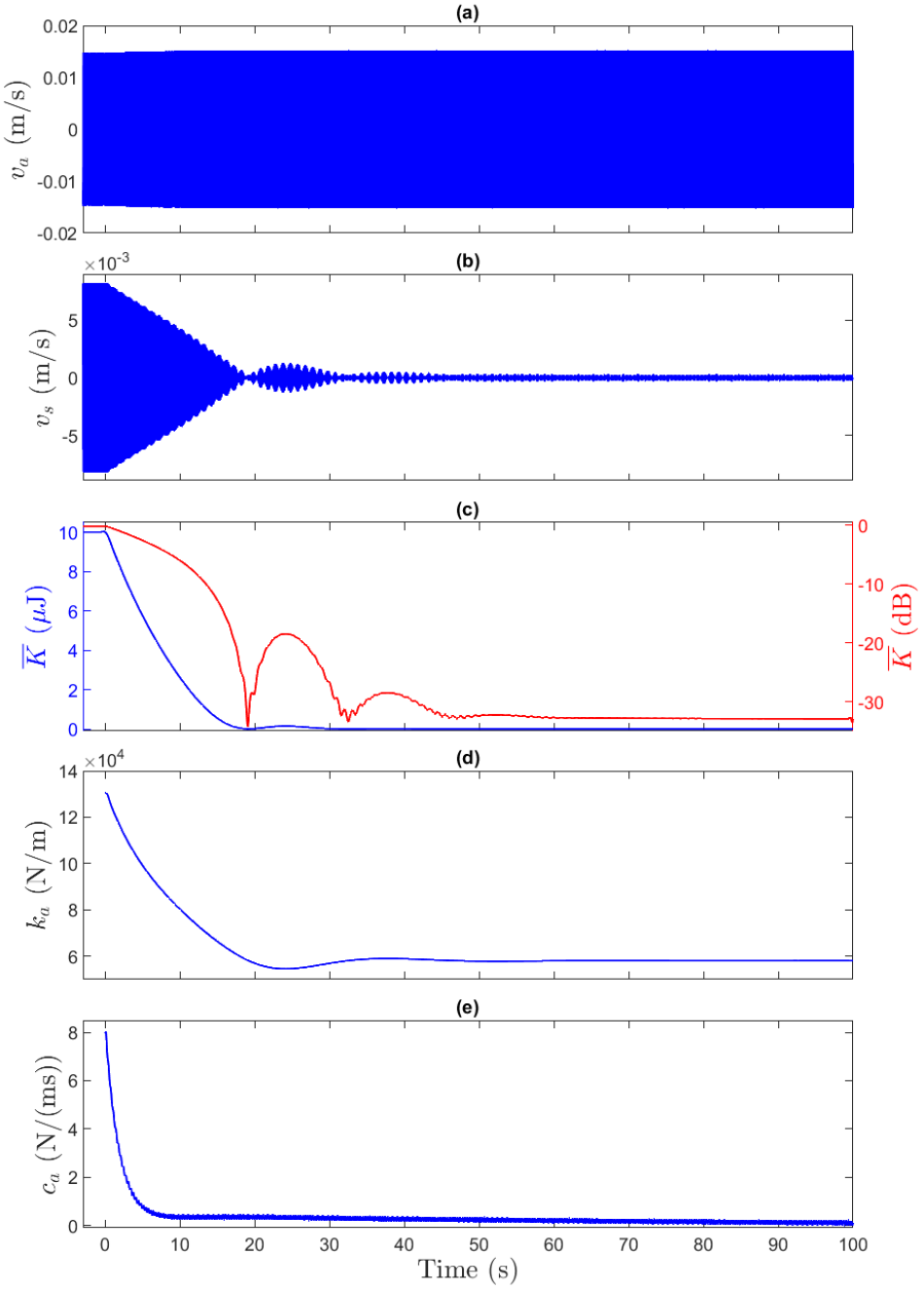

Figure 4: Time domain response of the system for the case 2: $\omega_0 = \omega_s$. (a) velocity of the TVA mass, (b) velocity of the structure mass, (c) time-average kinetic energy absolute value (blue line) and dB reduction with reference to its initial value (red line), (d) stiffness of the TVA, and (e) damping of the TVA.

Figures 3, 4, 5 present the time history plots during a span of 100 seconds for cases 1, 2, 3. More specifically the plots show: (a) the velocity of the TVA mass v_a, (b) the velocity of the structure mass v_s, (c) the time-average kinetic energy $\overline{K}$, (d) the stiffness k_a and (e) the damping c_a of the TVA. The time-average kinetic energy plot shows both the value in linear scale (blue line – left hand side scale) and the reduction value with respect to the initial value expressed in a dB (red line - right hand side scale). All simulations were carried out in such a way as during the initial 3 seconds, the extremum seeking controller is not working; and it is activated at $t = 0$ s. Considering first Figure 3 for case 1, in plot (a), it can be seen that the velocity of the absorber v_a starts with a low amplitude and, as the controller starts working, it constantly increases its value until reaching a maximum at around 67 s and then converges to a steady state value after 70 s. The

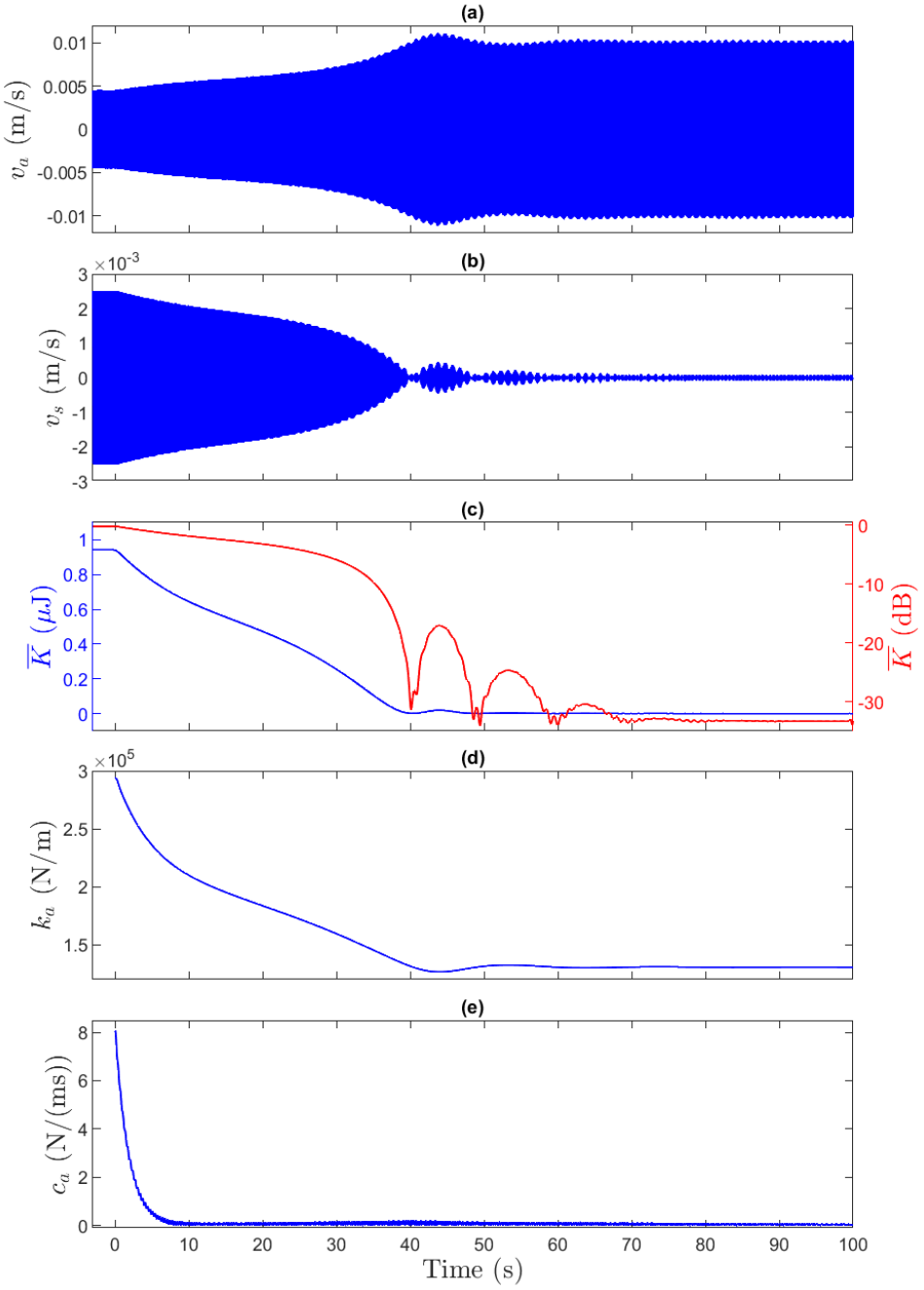

Figure 5: Time domain response of the system for the case 3: $\omega_0 = 1.5\omega_s$. (a) velocity of the TVA mass, (b) velocity of the structure mass, (c) time-average kinetic energy absolute value (blue line) and dB reduction with reference to its initial value (red line), (d) stiffness of the TVA, and (e) damping of the TVA.

velocity v_s of the structure mass shown in plot (b) presents exactly the opposite behavior: starting with its maximum value it decreases constantly, at a lower rate during the first 50 s and much faster between 50 s and 67 s, to then converge to a steady state minimum at around 70 s. Plot (c) shows that, when the controller is activated, the time-average kinetic energy always decreases, although at different rates, until converging to a minimum value at around 67 s. The red line shows that the greater reduction is achieved during the last 15 s in which a reduction of around 15dB is attained. The controller achieves a reduction of around 17 dB in this configuration. Plots (d) and (e) show that, during the first 5 seconds, the stiffness k_a and damping c_a varies rapidly towards the optimal values and then, during the following 5 sections, varies at a lower rate. After these 10 s, the stiffness continues in an almost constant rate and reaches its optimum value at around

67 s. Instead, the damping slowly starts to increase its convergence rate, with the highest rate in the last 15 s, which is also consistent with the rapid reduction of the kinetic energy in this interval. Overall, as expected for a TVA set to control tonal disturbances, the damping tends to zero.

Figure 4 presents the time histories of the five parameters for case 2, that is, when the forcing frequency matches the natural frequency of the hosting system. In this case, plot (a) shows little variation for the velocity of the TVA, which already from the beginning has a relatively high value. Plot (b) shows a fast decrease of the velocity of the hosting system mass, reaching its minimum value in less than 20 s. Plot (c) shows a rapid reduction of the time-average kinetic energy, consistent with the behavior of v_s. The mean kinetic energy reduction is around 32 dB in this case. The evolution of the TVA stiffness presented in plot (d) is consistent with that shown in the previous plot. Indeed, convergence occurs in less than 20 s, with little overshoot between 20 s and 30 s, which explains the increments in v_s and K during this time interval. Plot (e) shows the evolution of the TVA damping, which in less than 10 s rapidly converges to a small value and then tends to zero. These plots show that, for this condition, the control strategy has a much faster convergence rate, reaching a significant control effect in less than 20 s and steady state conditions at 40 s.

Figure 5 presents the time histories of the five parameters for case 3, that is, when the forcing frequency is 50% larger than the natural frequency of the hosting system. Plot (a) shows that the TVA mass is already moving with an intermediate velocity when the controller is activated and then slowly increases until reaching a maximum at around 55 s to finally reach a steady state condition after 60 s. Plot (b) shows that the velocity of the hosting system mass has the opposite behavior. More specifically, it decreases its value when the controller is activated and reaches a minimum at 50 s, where there a short oscillation followed by a steady state behavior. Plot (c) with time-average kinetic energy is consistent with the v_s plot, and thus reaches its lower vale at 55 s. In this case, the total reduction of the time-averaged kinetic energy is also around 32 dB. Plot (d) shows the evolution of the TVA stiffness, which after a fast convergence rate in the first 10 s, converges at an almost constant rate with little overshoot and reaching steady state condition in less than a minute. Plot (e) shows a rapid convergence of the TVA damping, which tends to zero in less than 10 s and remains low for the rest of the simulation.

Additional simulation analyses have shown that a particular condition can occur for cases 1 and 3, when the initial guess of the stiffness sets the TVA natural frequency in between the system natural frequency and the forcing frequency. In this case, the extremum seeking algorithm has a much longer convergence time. This is related to the higher velocity of the structure in the initial configuration, which induces the algorithm to drive the TVA damper c_a to a bigger value. The increased damping reduces the gradient for the tuning of k_a, thus its convergence speed. Eventually, with the convergence of TVA stiffness k_a, such that the TVA natural frequency is in the vicinity of the forcing frequency; the damping effect is overrun by the resonant absorber, thus, the extremum seeking drive the TVA damping c_a towards zero.

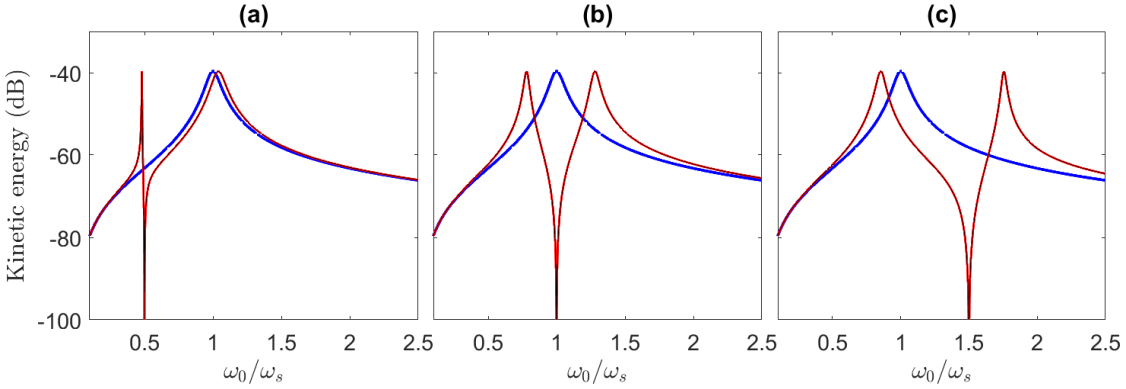

Figure 6: Spectra of the kinetic energy of the SDOF hosting system without the TVA (thick solid blue line), with the TVA implementing the theoretical optimal stiffness and damping values (solid red line) and the stiffness and damping values found with the extremum seeking algorithm (faint solid black line). (a) Case 1: $\omega_0 = 0.5\omega_s$, (b) Case 2: $\omega_0 = \omega_s$, and (c) Case 3: $\omega_0 = 1.5\omega_s$.

Figure 6 presents the spectra of the kinetic energy of the SDOF hosting system without the TVA (thick solid blue line), with the TVA implementing the theoretical optimal stiffness and damping values (solid red line) and the stiffness and damping values found with the extremum seeking algorithm (faint solid black line). Plot (a) show the results for the first case, plot (b) for the second case and plot (c) for the third case. These plots show that the vibration control performance obtained with the extremum seeking algorithm is very close to the optimal control derived using the theoretical optimal TVA stiffness and damping parameters.

3.2 Extremum seeking algorithm convergence analysis

This section presents a parametric analysis on how the 6 parameters that characterize the extremum seeking tuning algorithm may affect the stability and performance of the controller. In this simulation study the damping component c_a of the TVA is set to a very low constant value equal to 0.01 Ns/m. This means that there is only one tuning loop active, which searches for the optimum stiffness value.

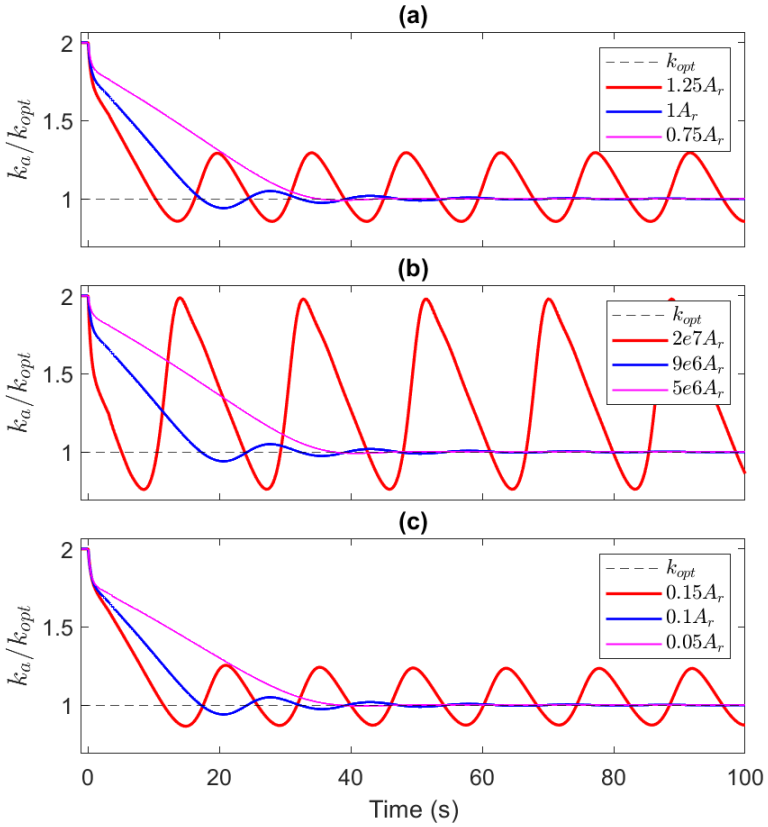

Figure 7: Effects of (a) the ripple amplitude A_r, (b) the tuning signal gain g_u and (c) the ripple gain g_r on the algorithm convergence to the optimal stiffness value (dashed black line). The baseline is the thin solid blue line, the thick solid red line corresponds to a value higher than the baseline and the faint solid magenta line to a value lower than the baseline.

As mentioned before, in total 6 parameters need to be configured for the extremum seeking algorithm: 3 parameters concerning amplitudes or gains and 3 referred to frequencies. Figure 7 shows the plots regarding the effect of the ripple amplitude A_r, the tuning signal gain g_u and the ripple gain g_r. Instead, Figure 8 presents the plots regarding the effect of the ripple frequency ω_r, the high-pass filter cut-off frequency ω_{hp} and the low-pass filter cut-off frequency ω_{lp}. The values shown in these figures are normalized with respect to the ripple amplitude A_r in Figure 7 and to the forcing frequency ω_0 in Figure 8. In both figures, the blue solid line stands for a configuration that achieves good control performance and is used as a baseline for comparison with higher (thick solid red line) and lower (faint solid magenta line) values of the considered

parameter. The constant value indicated by the dashed blackline represents the optimum stiffness value for the absorber.

Plot (a) in Figure 7 shows that increasing the ripple amplitude reduces the algorithm convergence time, but if the amplitude increases more than a certain threshold, the stability of the extremum seeking control is compromised. Plots (b) and (c) suggest that the same is true for the gains g_u and g_r; higher gain values translate into faster convergence, but too high values lead to instability.

Plot (a) of Figure 8 depicts the effect of the ripple frequency on the convergence behavior. An increase on the ripple frequency ω_r, produces similar results as the increase on the ripple amplitude, A_r, i.e., the convergence speed is increased but can also compromise the stability of the controller. Plot (b) shows that increasing the high-pass filter cut-off frequency ω_{hp} has the opposite effect, it reduces the speed of convergence and increases the stability of the system. Finally, Plot (c) indicates that increasing the low-pass filter cut-off frequency ω_{lp} produces a similar effect has increasing the high-pass cut-off frequency ω_{hp}.

As in most tuning strategies, a trade-off must be established to achieve good performance in a reasonable time without compromising the stability of the control system. In this study it was found that a proper implementation of the algorithm needs a careful choice of: first, the ripple signal frequency, second, the high-pass and, third, low-pass filters cut-off frequencies. After these frequencies are found to produce a stable and convergent algorithm, the gains can be increased to boost the convergence speed. It is also important to mention that, when the two TVA parameters are being tuned simultaneously, the ripple signals of each tuning loop should have different ripple frequency.

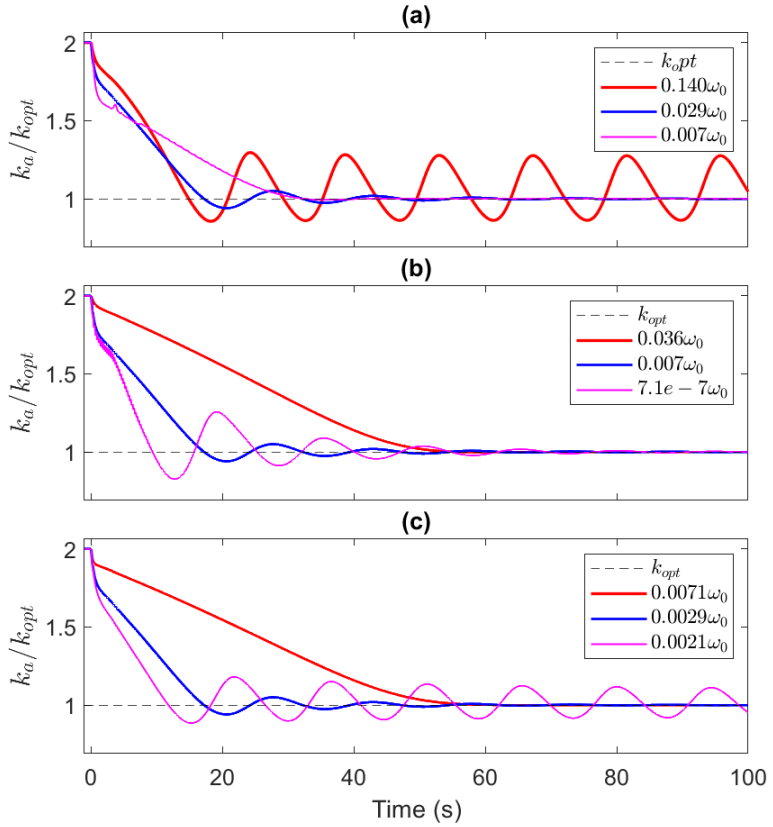

Figure 8: Effect of (a) the ripple frequency ω_r, (b) the high pass filter frequency and (c) the low pass filter frequency on the algorithm convergence to the optimal stiffness value (dashed black line). The baseline is the thin solid blue line, the thick solid red line is for a value higher than the baseline and the faint solid magenta line is for a value lower than the baseline.

4 Conclusions

This paper has presented a simulation study on the implementation of a tuning strategy for the stiffness and damping components of a TVA to control the response of a SDOF mechanical system subject to a harmonic force. The tuning strategy employs an extremum seeking algorithm that uses as a cost function the kinetic energy of structure and is implemented to search for both the TVA optimal stiffness and optimal damping simultaneously. Three cases were considered, that is when the harmonic force frequency is lower, equal, and higher than the natural frequency of the structure. Simulation results show that the extremum seeking algorithm converges to the optimum parameters in around 65 s, 20 s, and 50 respectively; achieving kinetic energy reductions of the order of 17 dB to 33 dB. A parametric study has also been presented to give insights on how the configuration of the parameters that characterise the extremum seeking algorithm impact on the convergence speed and stability of the algorithm itself. The proposed system needs little information of the hosting mechanical system, as opposed to classical tuneable vibration absorbers, and shows good control performance for tonal excitations.

References

[1] P. Watts, "On a method of reducing the rolling of ships at sea.," 1883, vol. 24, pp. 165–90.

[2] H. Frahm, "Device for damping vibrations of bodies," US989958A

[3] J. Ormondroyd and J. P. Den Hartog, "The theory of the Dynamic Vibration Absorber," *Journal of Applied Mechanics*, vol. 50, no. 7, pp. 9–22, 1928.

[4] J. Q. Sun, M. R. Jolly, and M. A. Norris, "Passive, Adaptive and Active Tuned Vibration Absorbers—A Survey," *Journal of Vibration and Acoustics*, vol. 117, no. B, pp. 234–242, Jun. 1995, doi: 10.1115/1.2838668.

[5] S. Krenk and J. Høgsberg, "Tuned mass absorber on a flexible structure," *Journal of Sound and Vibration*, vol. 333, no. 6, pp. 1577–1595, Mar. 2014, doi: 10.1016/j.jsv.2013.11.029.

[6] D. J. Mead, *Passive vibration control*. Chichester: John Wiley & sons, 2000.

[7] N. W. Hagood and A. von Flotow, "Damping of structural vibrations with piezoelectric materials and passive electrical networks," *Journal of Sound and Vibration*, vol. 146, no. 2, pp. 243–268, Apr. 1991, doi: 10.1016/0022-460X(91)90762-9.

[8] S. Wu, "Piezoelectric shunts with a parallel R-L circuit for structural damping and vibration control," San Diego, CA, May 1996, pp. 259–269. doi: 10.1117/12.239093.

[9] S. O. R. Moheimani and A. J. Fleming, *Piezoelectric transducers for vibration control and damping*. London: Springer, 2006.

[10] N. Alujević, I. Tomac, and P. Gardonio, "Tuneable vibration absorber using acceleration and displacement feedback," *Journal of Sound and Vibration*, vol. 331, no. 12, pp. 2713–2728, Jun. 2012, doi: 10.1016/j.jsv.2012.01.012.

[11] G. Zhao, N. Alujević, B. Depraetere, and P. Sas, "Dynamic analysis and $\mathscr{H}_2$ optimisation of a piezo-based tuned vibration absorber," *Journal of Intelligent Material Systems and Structures*, vol. 26, no. 15, pp. 1995–2010, Oct. 2015, doi: 10.1177/1045389X14546652.

[12] D. Casagrande, P. Gardonio, and M. Zilletti, "Smart panel with time-varying shunted piezoelectric patch absorbers for broadband vibration control," *Journal of Sound and Vibration*, vol. 400, pp. 288–304, Jul. 2017, doi: 10.1016/j.jsv.2017.04.012.

[13] C. Paulitsch, P. Gardonio, and S. J. Elliott, "Active Vibration Damping Using an Inertial, Electrodynamic Actuator," *Journal of Vibration and Acoustics*, vol. 129, no. 1, pp. 39–47, Feb. 2007, doi: 10.1115/1.2349537.

[14] A. J. Fleming and S. O. R. Moheimani, "Inertial vibration control using a shunted electromagnetic transducer," *IEEE/ASME Trans. Mechatron.*, vol. 11, no. 1, pp. 84–92, Feb. 2006, doi: 10.1109/TMECH.2005.863364.

[15] B. Yan, X. Zhang, Y. Luo, Z. Zhang, S. Xie, and Y. Zhang, "Negative impedance shunted electromagnetic absorber for broadband absorbing: experimental investigation," *Smart Mater. Struct.*, vol. 23, no. 12, p. 125044, Dec. 2014, doi: 10.1088/0964-1726/23/12/125044.

[16] X. Zhang, H. Niu, and B. Yan, "A novel multimode negative inductance negative resistance shunted electromagnetic damping and its application on a cantilever plate," *Journal of Sound and Vibration*, vol. 331, no. 10, pp. 2257–2271, May 2012, doi: 10.1016/j.jsv.2011.12.028.

[17] P. Gardonio, E. Turco, A. Kras, L. D. Bo, and D. Casagrande, "Semi-active vibration control unit tuned to maximise electric power dissipation," *Journal of Sound and Vibration*, vol. 499, p. 116000, May 2021, doi: 10.1016/j.jsv.2021.116000.

[18] S. H. Kamali, M. Moallem, and S. Arzanpour, "Self-Tuning Active Tuned Mass Damper Utilizing Constrained Multi-Variable Sliding Mode Extremum-Seeking," in *2018 IEEE Conference on Control Technology and Applications (CCTA)*, Copenhagen, Aug. 2018, pp. 127–131. doi: 10.1109/CCTA.2018.8511338.

[19] P. Gardonio, G. Konda Rodrigues, L. Dal Bo, and E. Turco, "Extremum seeking online tuning of a piezoelectric vibration absorber based on the maximisation of the shunt electric power absorption," *Mechanical Systems and Signal Processing*, vol. 176, p. 109171, Aug. 2022, doi: 10.1016/j.ymssp.2022.109171.

[20] K. B. Ariyur and M. Krstić, *Real time optimization by extremum seeking control*. Hoboken, NJ: Wiley Interscience, 2003.

[21] I. I. Ostrovskii, "Extremum regulation," *Automatic and remote control*, vol. 18, p. 1957, 907 900.

[22] I. S. Morosanov, "Method of extremum control," *Automatic and remote control*, vol. 18, pp. 1077–1092, 1957.

[23] M. Krstić, "Performance improvement and limitations in extremum seeking control," *Systems & Control Letters*, vol. 39, no. 5, pp. 313–326, Apr. 2000, doi: 10.1016/S0167-6911(99)00111-5.

[24] R. W. Clough and J. Penzien, *Dynamics of structures*, 2nd ed. New York: McGraw-Hill, 1993.